



DIRECT SEISMIC LOSS ESTIMATION METHODOLOGY WITH AN APPLICATION TO A PRECAST BUILDING

A. Babič⁽¹⁾, M. Dolšek⁽²⁾

⁽¹⁾ Assistant, University of Ljubljana, Faculty of Civil and Geodetic Engineering, anze.babic@fgg.uni-lj.si

⁽²⁾ Professor, University of Ljubljana, Faculty of Civil and Geodetic Engineering, matjaz.dolsek@fgg.uni-lj.si

Abstract

In the paper, a methodology for the seismic loss estimation is briefly presented and applied to a precast building. The loss estimation methodology consists of the hazard analysis, response history analysis, damage history analysis, restoration analysis and loss analysis. The damage history analysis enables precise simulation of the restoration measures, which can then be used for direct loss estimation without duplication of restoration measures or consideration of restoration measures that are not actually needed. Moreover, the damage of components that are considered in the mechanistic model of the building is simulated directly from the response history analysis. On the other hand, the damage of components which are not considered in the mechanistic model of the building is estimated by utilizing building's components fragility functions. The uncertainty of damage for a given value of intensity measure is considered by defining several building simulations and using each of them in various nonlinear response history analyses for a set of hazard consistent ground motion records.

The methodology is applied to a precast reinforced concrete warehouse building located in Slovenia. For the purpose of this application, a three-dimensional mechanistic model of the building was developed. The model contained structural as well as non-structural components. The results of the loss estimation are presented in terms of the collapse risk, expected annual loss and loss curve. The mean annual collapse frequency amounted to 1.8×10^{-3} , which is much more than expected for code-conforming buildings. The expected annual loss was equal to 0.26% of the cost of a new building including the cost of contents. A large part of the expected annual loss (80%) originated from the collapse cases. This was also reflected in the shape of the loss curve, which showed a pronounced jump in losses at frequencies close to the evaluated frequency of collapse.

Keywords: loss estimation; precast reinforced concrete building; collapse risk; expected annual loss; loss function

1. Introduction

Seismic loss estimation is a powerful tool which can be used in the lifecycle cost-benefit analysis [1], as well as in other risk-informed evaluation tools [2, 3]. The most widely used approach for seismic loss estimation is the PEER approach [4], which is also supported by a comprehensive database of fragility and loss functions.

In the PEER approach, the loss functions are defined at the level of component type, by prescribing a list of restoration measures (*RM*s) for the given damage state (*DS*) and assigning the losses (*L*s) to these *RM*s. In this approach, the lists of *RM*s are indirectly considered through *DS*-based loss functions, which can cause duplication of *RM*s or consideration of *RM*s that are not relevant for the component and simulation at hand. Furthermore, although the PEER methodology considers correlation between the outcomes within each step of the loss estimation, it neglects the correlation between the outcomes of the response history analysis and damage analysis, which occurs because the uncertainty in the capacity of a building component simultaneously affects the damageability of the component as well as the response history of the entire building [5].

The above issues can be especially relevant in cases of buildings that were not addressed in the development and validation of the PEER methodology. For example, PEER methodology was not yet applied to the precast reinforced concrete buildings that are commonly used in Europe. They are characterized by very slender columns, hinged connections between columns and beams, and precast cladding panels that are conventionally considered as non-structural components although they can significantly affect the seismic



response [6]. Additionally, the value of industrial equipment often exceeds the cost of construction of such buildings.

In this paper, a loss estimation methodology that addresses the challenges mentioned above is presented and applied to a precast building typical for Europe. The methodology is based on direct simulation of *RMs*, which enables assigning different *RMs* to components that are of the same type and experience the same level of damage. Moreover, the *DSs* of the components that are simulated in the mechanistic model of the building are simulated directly from the response history analysis, which means that the results of the response history analysis and damage analysis are inherently consistent. The methodology is described in Section 2, while its application is presented in Section 3. Conclusions are given in Section 4.

2. Description of the loss estimation methodology

In the proposed methodology, the loss is estimated based on direct simulation of *RMs*. The simulations are, however, divided into a mechanistic and a non-mechanistic simulation (Fig. 1). The mechanistic simulation comprises physics-based analyses, which includes both the response history analysis of all the components that have an essential effect on the building's engineering demand parameters (*EDPs*) as well as the corresponding damage history analysis (Fig. 1a). The components that essentially affect the building's *EDPs* are denoted as primary components. The outcomes of the response history and damage history analysis of primary components are, respectively, the history of *EDPs* and the history of the occurrence of *DSs* of primary components. The *DSs* occurrence history is expressed in the form of a damage history matrix, which contains information regarding the occurrence times of all *DSs* identified in the damage history analysis of primary components. The analyses are explained in more detail in Section 2.1.

Not all components of the building are included in the response history analysis, due to their insignificant effect on the global seismic response. These components are termed secondary components. Consequently, damage history analysis of the secondary components is a part of the non-mechanistic simulation, which is performed by considering the *EDPs* and *DSs* of the primary components simulated in the preceding mechanistic simulation (Fig. 1b). The outcome of the damage history analysis of the secondary components is the *DSs* occurrence history of secondary components, which is expressed by updating the damage history matrix formed in the mechanistic simulation. The analysis is explained in more detail in Section 2.2.

The non-mechanistic simulation also includes the restoration analysis and loss analysis (Fig. 1b), which are non-mechanistic by nature. In these analyses, no distinction is made between the primary and secondary components. The outcome of the restoration analysis is the list of *RMs*, while the outcome of the loss analysis is a single loss value (i.e. the total loss L_T). The analyses are explained in more detail in Section 2.3.

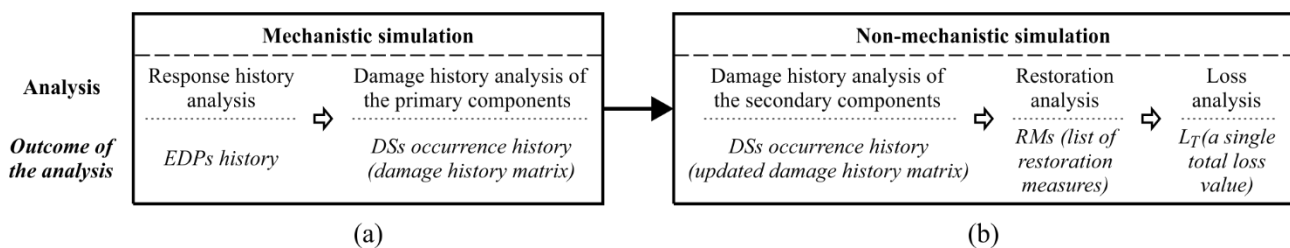


Fig. 1 – The division of a single loss simulation to (a) the mechanistic simulation and (b) the non-mechanistic simulation.

In order to consider the modelling uncertainties and record-to-record randomness, several loss simulations are performed at various levels of intensity measure (*IM*). However, before performing the simulations, input data corresponding to both types of simulations is processed. Based on the division between the mechanistic and non-mechanistic simulation, input parameters are classified as mechanistic or non-mechanistic input parameters, respectively. It is possible that some of the mechanistic and non-mechanistic input parameters could be considered deterministic (i.e. constant values) and that some should be considered



uncertain in order to estimate the dispersion of L_T with sufficient accuracy. Processing of input data involves the determination of samples of uncertain parameters. Thus, N_m samples of mechanistic and N_n samples of non-mechanistic input parameters are generated and used, respectively, in mechanistic and non-mechanistic simulations. Any suitable method can be used to generate these samples. A possible choice is the Latin Hypercube Sampling (LHS) method [7] in combination with the simulated annealing algorithm [8], which has been used before in the field of earthquake engineering [9].

The record-to-record randomness is accounted for at each level of IM by N_a ground motions. For each ground motion, $N_m \times N_n$ loss simulations are performed as shown by the algorithm presented in Fig. 2. Thus, each combination of the mechanistic and non-mechanistic simulation results in a unique damage history matrix (Section 2.2), a unique list of RM s (Section 2.3), and the resulting total loss L_T (Section 2.3). For each loss simulation, the collapse is also indicated in the damage history matrix if identified in the mechanistic part of the simulation. By considering all the ground motions, the probability of building's collapse conditional to the level of IM can be calculated. The above process is performed for each of the N_a ground motions which are scaled to N_i levels of IM . Thus, N_i collapse probabilities and N_i loss samples are obtained. For each level of IM , the sample size of losses L_T is equal to $N_a \times N_m \times N_n$.

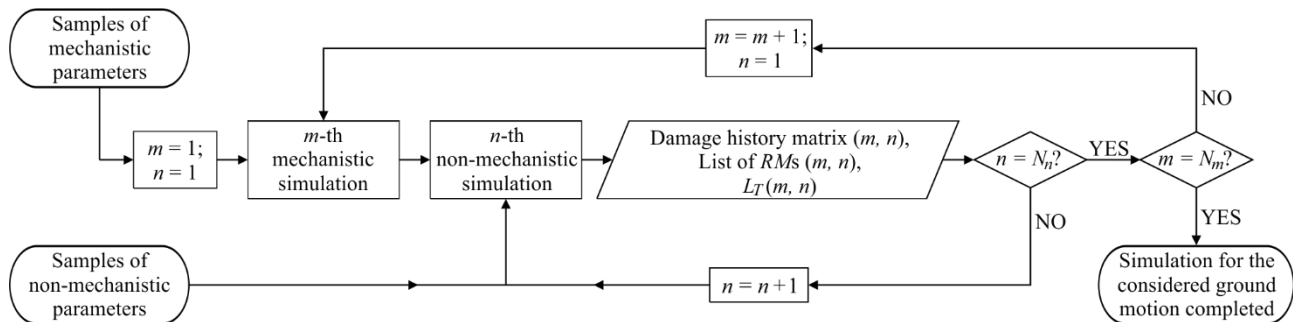


Fig. 2 – The algorithm for the realization of a sample of mechanistic and non-mechanistic simulations for a specific ground motion.

Based on the collapse probabilities and by utilizing a suitable regression method (e.g. the maximum likelihood method), the building's collapse fragility function is derived and coupled with the seismic hazard curve in order to calculate the building's mean annual collapse frequency $\lambda(C)$. Moreover, based on the loss samples, the mean vulnerability function is derived. This is done by first calculating the expected L_T for each of the N_i levels of IM , and then interpolating between these expected values of L_T . However, vulnerability functions are also determined for different percentiles of the loss distribution. Each such vulnerability function is derived by means of interpolation between the same percentiles of L_T . Finally, based on the vulnerability functions and by considering the seismic hazard curve, the expected annual loss EAL and the loss curve $\lambda(L_T > l_T)$, which indicates the frequency λ of exceedance of loss l_T , are obtained.

2.1 Response history analysis and damage history analysis of primary components

The response history analysis is performed to obtain the history of any EDP that can be simulated by the mechanistic model of the building and considered an appropriate measure for direct estimation of damage in any of the building's components (primary or secondary). The mechanistic model should at least include the vital structural components. However, in the case where the non-structural components significantly affect the seismic response, those components should also be included in the mechanistic model.

The history of $EDPs$ of the primary components is used directly to determine the DS s of the primary components. For example, if the EDP in a column exceeds deformation related to the concrete spalling, the DS corresponding to the spalling is assigned to that column. Thus, the definition of the onset of DS s is deterministic. However, this does not mean that the occurrence of a DS itself is deterministic. For instance, in the case where the DS is defined deterministically by the spalling deformation, the spalling deformation itself



can be considered uncertain, as in the case of the presented example (Section 3). The effect of the uncertainty in the *DSs* can thus be considered by performing a sufficient number of mechanistic simulations. The advantage of such a damage analysis is that the *DSs* observed in the primary components are inherently consistent with the results of the response history analysis.

The *DSs* that are identified during the damage history analysis of the primary components are systematically presented by the damage history matrix (Fig. 3a). The damage history matrix consists of three columns that represent the occurrence time of the *DS*, the *ID* of the damaged component, and the *ID* of the *DS*. The occurrence time of a *DS* is determined as the time at which the capacity of the *DS* (denoted as *engineering capacity parameter – ECP*) is first exceeded by the corresponding demand (i.e. *EDP*). Moreover, if the collapse of the building is identified, its occurrence and the corresponding time instance t_c is indicated in the last row of the damage history matrix (Fig. 3a).

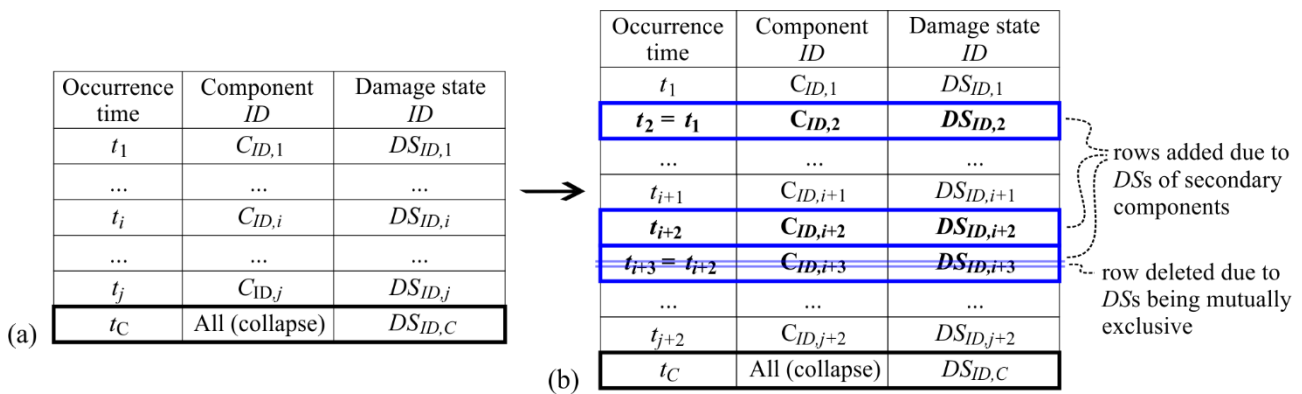


Fig. 3 – An example of the damage history matrix in the case of collapse: (a) with sole consideration of the primary components, and (b) with additional consideration of the secondary components. Notations $C_{ID,i}$ and $DS_{ID,i}$ refer to the *ID* of the component and the *ID* of the *DS* from the i -th row of the damage history matrix.

2.2 Damage history analysis of secondary components

The *DSs* of the secondary components are simulated in two different ways. First, the *DSs* are simulated based on the conventional approach. In this case, the capacity corresponding to the given *DS* (i.e. *ECP*) is defined and compared to the appropriate demand. The *ECPs* of the given component that correspond to the designated *DSs* are defined by utilizing the *EDP*-based fragility functions (e.g. ATC, 2012), while the demand is approximated by the *EDP* of the closest primary component obtained in the response history analysis. The *DS* is considered to be reached if $EDP \geq ECP$.

In addition to the *DSs* of secondary components that are simulated based on the fragility functions, the damage caused by domino effects is also simulated. For this simulation, it is necessary to pre-identify potential interactions between the *DSs*. Each such interaction is defined by the triggering component (i.e. the trigger) and the corresponding trigger *DS*, and by the targeted component (i.e. the target) and the corresponding target *DS*. An example of such an interaction between the *DSs* is the collapse of an equipment unit that is triggered by the overturning of an adjacent storage rack (Fig. 4a). The identification of all potential interactions between the *DSs* can be a complicated process. For this reason, the interactions are first *defined* at the level of a few component groups that consist of structurally and functionally similar components. Only then, the interactions at the level of individual components are automatically *identified* based on the distance between the components that have the potential to act as triggers and components that can act as targets. With all the interactions identified, the simulation of *DSs* is performed by examining if the trigger *DS* has occurred in the trigger. If this is the case, the target *DS* is simply assigned to the target. Such simulation of *DSs* makes it possible to consider the interdependencies between the *DSs* that would be difficult to include solely by taking



into account the statistical correlation. Moreover, by considering a given *DS* as both a target *DS* and a trigger *DS*, it is possible to model multi-level domino effects.

The *DS*s of the secondary components are added to the damage history matrix of the primary components (Fig. 3b). The occurrence time of a given *DS* is equal to the time at which the *ECP* is first exceeded by the corresponding *EDP* (if the *DS* is simulated based on the conventional approach), or to the occurrence time of the trigger *DS* (if the *DS* is simulated based on the interactions between the *DS*s). Simultaneously to adding the *DS*s of the secondary components to the damage history matrix, the matrix is revised by deleting duplicated and mutually exclusive *DS*s (Fig. 3b). In the case of mutually exclusive *DS*s, only the *DS* that occurs first is kept in the matrix. Thus, the progression of damage throughout the earthquake is simulated for the secondary components as well.

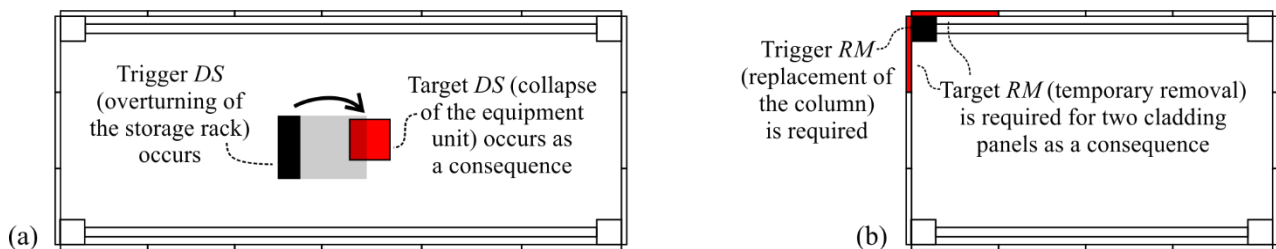


Fig. 4 – (a) an example of the interaction between *DS*s, and (b) an example of the interaction between *RMs* in a precast building.

2.3 Restoration analysis and loss analysis of all building components

The simulation of *RMs* is performed in two different ways. First, the *RMs* are simulated as direct consequences of the *DS*s that were stored in the damage history matrix. An example of such a *RM* is the replacement of a column due to its extensive damage.

However, some *RMs* require that other *RMs* are also performed. For instance, in the example presented in Section 3, the replacement of a column requires that the adjacent cladding panels are temporarily removed. For this reason, the *RMs* are also simulated by considering the interactions between the *RMs*. Such interactions are analogous to the interactions between the *DS*s in the sense that the occurrence of the trigger *RM* in a given building component (i.e. the trigger) causes the occurrence of the target *RM* in another, adjacent building component (i.e. the target). In the previous example, the trigger *RM* and the target *RM* would be the replacement of the column and the temporary removal of the cladding panel, respectively (Fig. 4b). In order to simplify the input for such simulation of *RMs*, the interactions between the *RMs* are first *defined* at the level of a few component groups and then automatically *identified* at the level of individual components based on the distances between the components that have the potential to act as triggers and components that can act as targets.

All the simulated *RMs* are stored in the list of *RMs*. Due to several possible sources of *RMs*, it is possible that a given *RM* on list of *RMs* is duplicated. This problem can be solved by simply removing all the *RMs* that are repeated. Moreover, it is possible that two *RMs* are incompatible (e.g. the temporary removal and the replacement of the same cladding panel). If this happens, the less severe *RM* (i.e. the temporary removal of the cladding panel from the previous example) is removed from the list of *RMs*.

The losses (*L*s) corresponding to individual *RMs* are then determined. It is foreseen that the *L*s are obtained from the *RM*-based loss functions that are defined as cumulative distribution functions of *L*, thus being analogous to the *DS*-based loss functions utilized in the PEER methodology [4]. However, the difference between the *RM*-based and *DS*-based loss functions is that in the former case, *L*s are calculated as direct consequences of *RMs* rather than estimated indirectly through the observed *DS*s. Finally, by summation of *L*s corresponding to all *RMs*, the total loss L_T is obtained.



3. Application of the loss methodology to a precast building

The investigated building is a single-story warehouse located in Ljubljana, Slovenia (Fig. 5a). It has a precast reinforced concrete structure (Figs. 5b, 5c and 5d), which consists of cantilever columns, longitudinal and transverse beams, and pi-slabs. The longitudinal (main) beams are pinned to the top of the columns by steel dowels and connect the columns in the direction of the longer inter-column span. The transverse beams are used to connect the perimeter columns in the direction of the shorter inter-column span. The pi-slabs connect the longitudinal beams in the direction perpendicular to their axis. The structural components that predominantly affect the seismic response of precast reinforced concrete structures similar to the structure of the analysed building are the columns and the dowel connections between the beams and columns [6]. The columns were designed [10] according to Eurocode 8 [11]. However, in the case of the dowel connections, no model for the calculation of the connection strength is provided in Eurocode 8. Therefore, the connections were designed [10] based on the state-of-the-practice approach, where the strength of the dowel connections is considered equal to the shear strength of the dowels themselves [6].

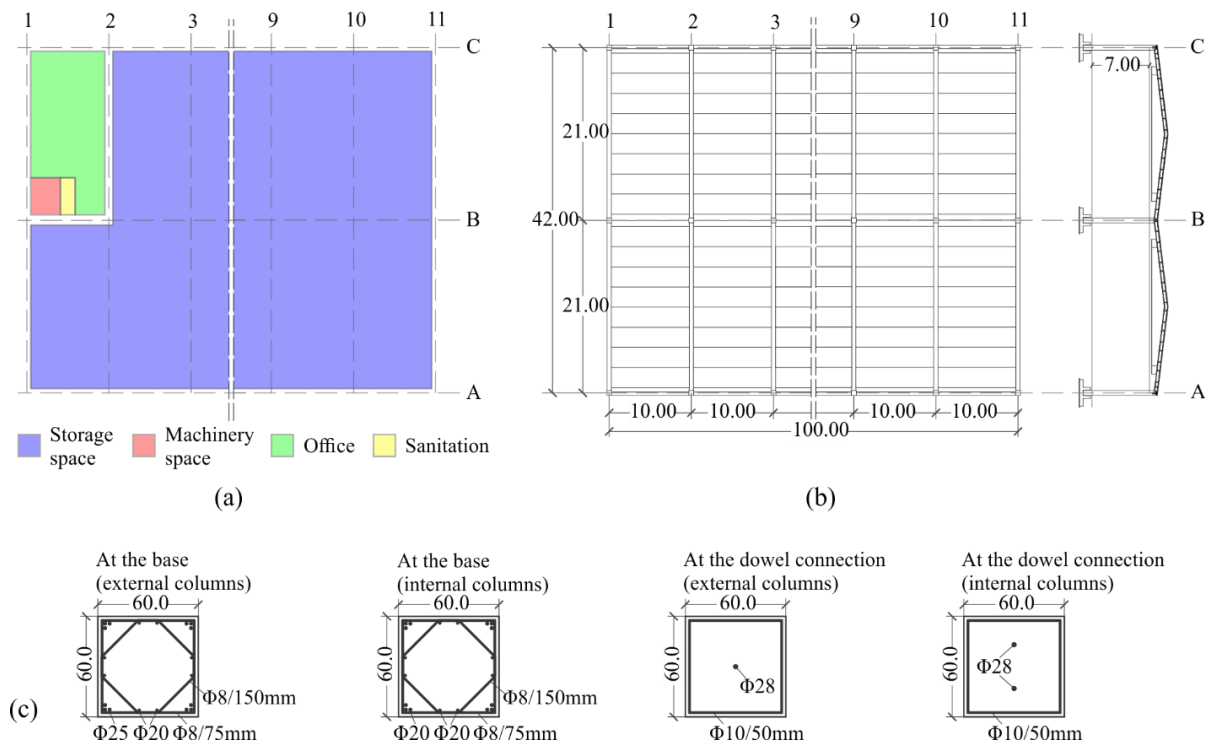


Fig. 5 – The investigated building: (a) the layout of the ground floor, (b) the plan view and the section view of the structure, and (c) reinforcement in the columns.

At the building's perimeter, vertical precast cladding panels, which are considered non-structural components, are attached to the longitudinal and transverse beams by special fastenings [12]. In addition to the structural and non-structural components, the stored equipment, storage racks and air handling unit are considered as the most valuable contents of the building. The cost of a new building amounts to approximately 3.7 million euro including the cost of contents.

According to the proposed methodology, the components of the building were divided into primary and secondary components. The primary components comprised columns, longitudinal and transverse beams, pi-slabs and cladding panels. The secondary components comprised foundation, flooring, roofing, suspended ceiling, partition walls, doors, gutters, lights, computer equipment, office equipment, ducts, diffusers, an air handling unit, stored equipment, storage racks, surveillance cameras, the construction pit and rugged installations. The restoration of the construction pit and rugged installations was only possible in the case of collapse of the building.



3.1 The mechanistic model of the building for response history analyses

A three-dimensional mechanistic model of the building was developed within the OpenSees platform [13] using the lumped-plasticity approach from a previous study [6]. By definition (Section 2), the primary components (i.e. the columns, longitudinal and transverse beams, pi-slabs and cladding panels) were considered in the model.

The columns were modelled as one-component lumped-plasticity elements with two independent rotational springs. The backbone curve and the hysteretic rules that approximately account for cyclic degradation of strength and stiffness [14], were considered. Longitudinal and transverse beams were modelled as elastic elements with concentrated masses at their endpoints. The connections between beams and columns were modelled by several zero-length elements connected in parallel in order to simulate the effect of the steel dowel, the friction between the corbel at the top of the column and the beam, and the impact between the column and the beam. It should be noted that the strength of the dowel connections was calculated by using a model [15], which was more realistic than that used in the design phase, since it had been developed only after the building had been designed. Moreover, the zero-length element that simulated the effect of the dowel was removed from the model during the analysis if the failure of the dowel was identified. In the case of the transverse beams, the failure of the dowel also indicated the removal of the beam itself, due to the insignificant contribution of friction to the overall strength of the beam-to-column connection. The effect of the pi-slabs was modelled by a very stiff elastic element.

The cladding panels are fixed at the base and at the top connected by fastenings to the beams. Thus the rocking of cladding panels is prevented, but the panels can still rotate at the base in the out-of-plane direction. The interaction between the panels and the longitudinal or transverse beam was modelled by zero-length elements that simulated the effect of the fastenings [12]. The node at the top of each panel contained one half of the panel's mass and moved freely in the out-of-plane direction, thus simulating the inertial forces due to the panel. The finite elements that were used to model a given panel were removed from the model during the analysis if the fastenings of that panel failed in either the in-plane or the out-of-plane direction. In addition, the panel was removed from the model if it was connected to a transverse beam that was, itself, removed from the model.

The uncertain mechanistic parameters included mass, damping ratio, material characteristics, modelling parameters corresponding to the response of the columns, and parameters related to the attachment of cladding panels that affected the response of the fastenings. Altogether 13 mechanistic input parameters were modelled by random variables. Modelling parameters of the columns were considered correlated. The correlation coefficients were obtained from a study by Ugurhan et al. [16].

3.2 Input parameters for the damage history analysis

The definition of *DSs* depended on the type of the component. In the case of primary components, the occurrence of *DSs* was directly defined by capacities (*ECPs*) that indicated the strength or deformation capacities of the component. In Table 1, an example of the definition of *DSs* is presented for cladding panels. Definition of *DSs* of other primary components can be found elsewhere [17].

Table 1 – The definition and simulation of *DSs* of cladding panels (example primary components)

<i>DS</i>	Description of the <i>DS</i>	Indication of the <i>DS</i> (<i>EDP</i> and the corresponding <i>ECP</i>)
<i>DS1</i>	Moderate damage in the fastenings	In-plane or out-of-plane displacement in the fastenings exceeding the in-plane or out-of-plane yield capacity, respectively
<i>DS2</i>	Dislocation and overturning of the panel due to failure of the fastenings or due to the dislocation of the supporting transverse beam	In-plane or out-of-plane displacement in the fastenings exceeding the in-plane or out-of-plane ultimate capacity, respectively; displacement in the dowel connection of the supporting transverse beam exceeding its capacity



The response of the primary components was also used as the indicator of building's collapse. Two types of collapse mechanisms were considered. The first type was associated with the total loss of bending strength in at least one column, while the second type was defined by the unseating of at least one longitudinal beam from the supporting column.

In the case of the secondary components, several *DSs* were simulated based on the comparison between *ECPs* and *EDPs*, whereby defining the *ECPs* based on the fragility functions from [4]. However, several *DSs* were also simulated based on their interactions with other *DSs*. The interactions between the *DSs* that were considered in the analysis were related to components dislocating from their support and consequently falling on the components below (e.g. ducting, lights or suspended ceiling falling on the equipment below), or to the overturning of components (e.g. cladding panels or storage racks overturning and falling on the adjacent equipment pieces). The definition of interactions between the *DSs* was based on the location and the size of the components. In Table 2, an example of the definition of *DSs* is presented for computer equipment. Observe that three *DSs* were simulated based on their interactions with other *DSs* (occurring in the suspended ceilings located above the equipment) and one *DS* was simulated based on the comparison between its *ECP* and the corresponding *EDP*. Definition of *DSs* of other secondary components can be found elsewhere [17].

Table 2 – The definition and simulation of *DSs* of computer equipment (example secondary components)

<i>DS</i>	Description of the <i>DS</i>	Simulation of the <i>DS</i> based on the comparison between <i>ECP</i> and <i>EDP</i>	Simulation of the <i>DS</i> based on an interaction with another <i>DS</i>
<i>DS1</i>	5% of equipment damaged due to the impact with the suspended ceiling tiles above	/	Triggered by a <i>DS</i> in suspended ceiling located above the equipment (5% of the ceiling tiles dislocated)
<i>DS2</i>	30% of equipment damaged due to the impact with the suspended ceiling tiles above	/	Triggered by a <i>DS</i> in suspended ceiling located above the equipment (30% of the ceiling tiles dislocated)
<i>DS3</i>	50% of equipment damaged due to the impact with the suspended ceiling tiles above	/	Triggered by a <i>DS</i> in suspended ceiling located above the equipment (50% of the ceiling tiles dislocated)
<i>DS4</i>	Failure of functionality (acceleration sensitive)	Fragility function: $\overline{PGA} = 0.4g, \beta_{PFA} = 0.5$	/

3.3 Input parameters for the restoration analysis and loss analysis

The *RM*s that were simulated as direct consequences of *DS*s were defined according to previous loss estimation studies, where the *DS*s had been linked to *L*s by assuming a default set of *RM*s [4, 18]. In those studies, the reported *RM*s are generic, while in the proposed methodology, *RM*s are directly simulated. However, the interactions between the *RM*s were also taken into account in order to appropriately simulate the temporary or permanent removal of components adjacent to the damaged components. For this purpose, it was necessary to define the distances between the components at which the interactions between the *RM*s could take place. These distances were defined partly based on [4] and partly based on engineering judgment. In Table 3, an example of the definition of *RM*s is presented for cladding panels. Definition of *RM*s of other components can be found elsewhere [17].



Table 3 – The definition and simulation of *RM*s, and the corresponding median *L*s of cladding panels (example component)

<i>RM</i>	Description of the <i>RM</i>	Simulation of the <i>RM</i> as a direct consequence of a <i>DS</i>	Simulation of the <i>RM</i> based on an interaction with another <i>RM</i>	$\bar{L} RM$ [€]
<i>RM1</i>	Repair of the fastenings	Due to <i>DS1</i> in the panel	/	100
<i>RM2</i>	Temporary removal of the panel	Due to <i>DS1</i> in the panel	Triggered by a <i>RM</i> in any column closer than 2.5 m (if only epoxy injection is required in the column) or 5 m (if the column needs to be partially or fully replaced)	350
<i>RM3</i>	Replacement of the panel	Due to <i>DS2</i> in the panel	/	4900

The *L*s corresponding to the *RM*s were considered uncertain and modelled by a truncated lognormal distribution. Their median values were estimated based on Slovenian cost databases [19] and the documents issued by the Slovenian government after the Posočje earthquakes [20]. The median *L*s for the example *RM*s are presented in Table 3. However, the dispersion parameters, as well as the minimum and maximum values, were based on expert judgement, due to the lack of studies on the dispersion of prices in Slovenia. The logarithmic standard deviation ranged from 0.15 to 0.5, while the minimum and maximum values differed from the median for ± 35 –60%.

3.4 Hazard analysis and ground motions used in the response history analyses

The hazard curve (Fig. 6a) was determined according to the methodology used in the development of seismic design maps in Slovenia [21]. The geometric mean of horizontal spectral accelerations at 1.6 s was used as the *IM*. The period of 1.6 s was selected because it is the yield period of the structure with mean characteristics.

The conditional spectrum approach [22] was used for the selection of 30 ground motions, which were used in the response history analyses ($N_a = 30$; Fig. 6b). All three ground-motion components were considered in the response history analyses because the occurrence of unseating of the beams from the columns in this type of precast buildings strongly depends on vertical accelerations [6].

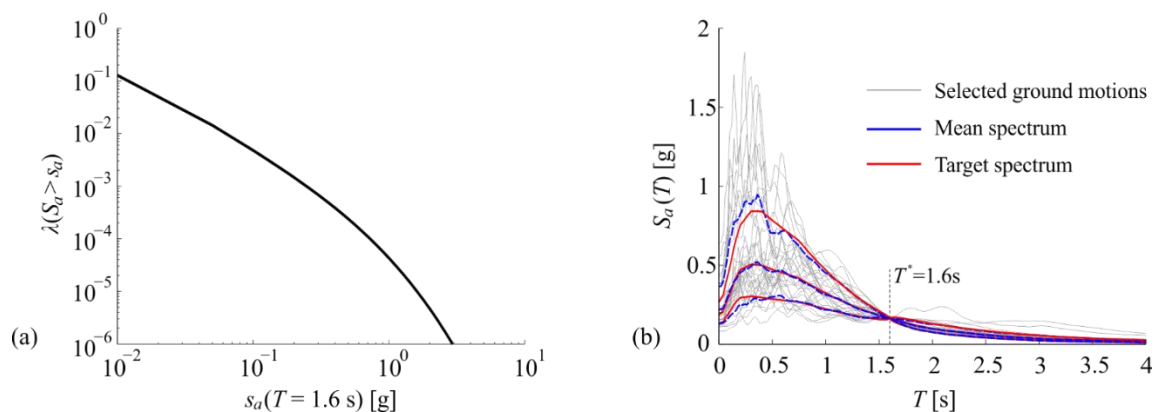


Fig. 6 – (a) Hazard curve and (b) the target spectra and the corresponding spectra of selected ground motions based on the geometric mean of spectral acceleration of horizontal ground-motion components.

3.5 Loss simulations and results of the loss estimation

The ground motions were scaled to 21 levels of *IM* ($N_i = 21$) ranging from 0.014 g to 0.77 g. For each ground motion and level of *IM*, 22500 loss simulations ($N_m \times N_n = 30 \times 750 = 22500$) were performed. The number of mechanistic simulations is equal to the number of ground motions. This is considered acceptable because the number of random mechanistic input parameters was intentionally limited to 13. However, many more



non-mechanistic simulations ($N_n = 750$) were performed because of the higher number of uncertain non-mechanistic input parameters (150) and low computational costs.

Based on the collapse probabilities observed from the mechanistic simulations and by using the maximum likelihood method, the collapse fragility function of the building (Fig. 7a) was derived. In combination with the hazard curve (Fig. 6a), the fragility function resulted in $\lambda(C)$ equal to 1.8×10^{-3} . Such a high value of $\lambda(C)$ can be attributed to the different models used for the calculation of the strength of the dowel connections which were used in the design phase and the estimation phase. It should be noted, however, that the model used in the estimation phase [15] is foreseen to be included in the new Eurocode [23]. This will provide the guidelines for the design of the dowel connections that is consistent with the capacity design principle, thus preventing the dowel connections from being the weak part of the structure.

However, based on the loss samples at the selected levels of IM , the vulnerability functions were derived. The mean vulnerability function, as well as the 10th and 90th percentile vulnerability functions, are presented in Fig. 7b. It can be observed that the confidence bands are quite wide. For example, if considering the 80 percent confidence level, the estimated L_T for a 1000-year event ($S_a = 0.23$ g) ranges between 1.4 and 4.5 million euro.

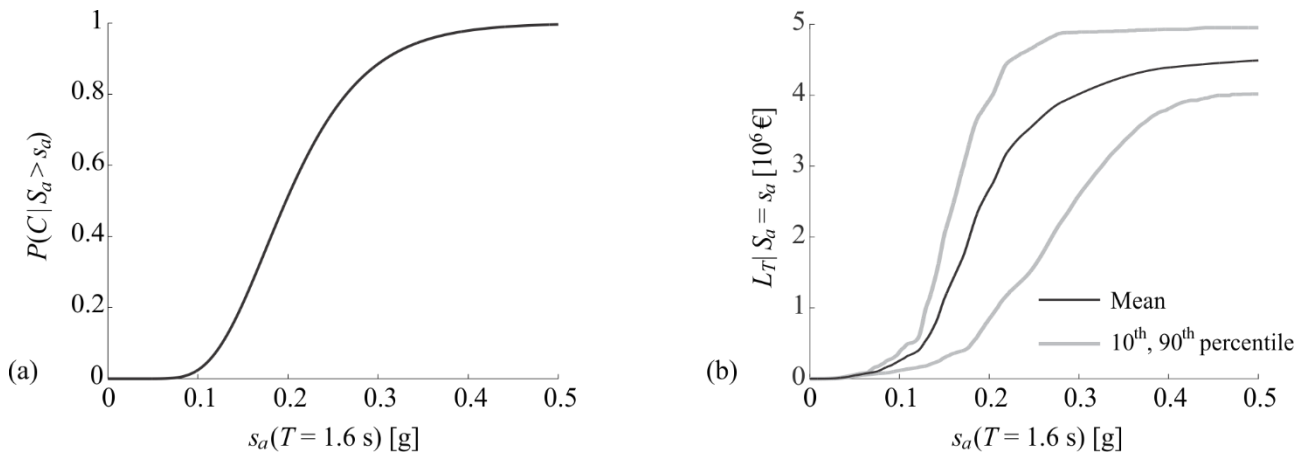


Fig. 7 – (a) collapse fragility function and (b) vulnerability functions of the building.

The large dispersion of L_T is also reflected in the conditional complementary cumulative distribution functions $P(L_T > l_T | S_a)$ (Fig. 8a). It can be observed that each such function exhibits a plateau where the probability $P(L_T > l_T | S_a)$ remains constant while L_T increases significantly. These plateaus divide the non-collapse cases (left from the plateau) from the collapse cases (right from the plateau). In the case of $S_a = 0.2$ g, for example (Fig. 8a), the plateau is at the probability of 55%, which also represents the probability of collapse at $S_a = 0.2$ g.

Finally, by combining the vulnerability functions with the hazard curve, the EAL and the loss curve $\lambda(L_T > l_T)$ were obtained. The EAL amounted to 0.26% of the cost of a new building including the cost of contents, which is a rather low value considering the high probability of collapse. However, this can be attributed to the low contribution of the non-collapse cases to the EAL (about 80% of the EAL originated from the collapse cases). The high contribution of the collapse cases to the overall losses is also reflected in the shape of $\lambda(L_T > l_T)$ (Fig. 8b), which shows a pronounced jump in losses at frequency values close to $\lambda(C)$.

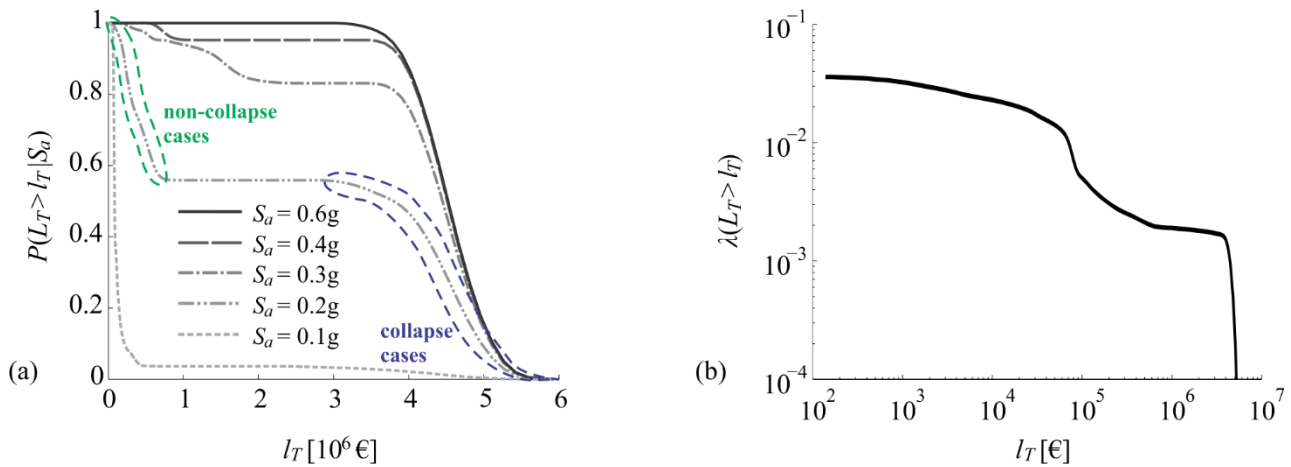


Fig. 8 – (a) Conditional complementary cumulative distribution functions of L_T for different levels of S_a (losses from the non-collapse and collapse cases are shown for $S_a = 0.2$ g) and (b) loss curve of the building.

4. Conclusions

In the paper, a seismic loss estimation methodology is briefly presented. It makes it possible to simulate losses directly from the restoration measures, which guarantees that the total loss is not overestimated due to duplication of restoration measures or consideration of generic restoration measures that are not actually required. Moreover, the methodology considers interactions between damage states and restoration measures, which enables incorporating, respectively, interdependencies between the damage states and between the restoration measures. Furthermore, the correlation between the seismic response analysis and damage analysis is simulated directly, which is achieved by performing damage history analysis as a part of the mechanistic simulation.

The proposed methodology can be used for improving insight into loss estimation. It is especially recommended in cases when a detailed mechanistic model of the building is available. However, the methodology can also serve as a basis for justifying simplifications in the development of practice-oriented loss estimation procedures. Moreover, by introducing restoration analysis into the methodology, it represents a step towards the improvement of the resilience estimation, which is significantly affected by the restoration process.

The main focus of the paper was to demonstrate the loss estimation methodology by estimating the collapse risk and the economic loss for a warehouse precast building. The mean annual collapse frequency amounted to 1.8×10^{-3} , while the expected annual loss was equal to 0.26% of the cost of a new building including the cost of contents. A large part of the expected annual loss (80%) originated from the collapse cases. This was also reflected in the shape of the loss curve, which showed a pronounced jump in losses at frequencies close to the frequency of collapse.

5. Acknowledgements

The research presented in this paper is based on work financed by the Slovenian Research Agency. This support is gratefully acknowledged.

6. References

- [1] Wen YK, Kang YJ (2001): Minimum building life-cycle cost design criteria, I: Methodology. *ASCE Journal of Structural Engineering*, **127** (3), 330-337.
- [2] Esposito S, Stojadinović B, Babič A, Dolšek M, Iqbal S, Selva J, Broccardo M, Mignan A, Giardini D (2020): Risk-Based Multilevel Methodology to Stress Test Critical Infrastructure Systems. *Journal of Infrastructure Systems*, **26** (1). (in press.)



- [3] Babič A, Dolšek M (2019): A five-grade grading system for the evaluation and communication of short-term and long-term risk posed by natural hazards. *Structural Safety*, **78**, 48-62.
- [4] ATC (2012). FEMA P-58-1 - Seismic performance assessment of buildings: Volume 1 - Methodology. Redwood City.
- [5] Bradley BA, Lee DS (2010): Component correlations in structure-specific seismic loss estimation. *Earthquake Engineering and Structural Dynamics*, **39** (3), 237-258.
- [6] Babič A, Dolšek M (2016): Seismic fragility functions of industrial precast building classes. *Engineering Structures*, **118**, 357-370.
- [7] McKay MD, Conover WJ, Beckman RA (1979): Comparison of three methods for selecting values of input variables in the analysis of output from a computer code. *Technometrics*, **21** (2), 239-245.
- [8] Vorechovsky M, Novak D (2003): Statistical correlation in stratified sampling. *International Conference on Applications of Statistics and Probability in Civil Engineering ICASP 9*, San Francisco, CA, USA.
- [9] Dolšek M (2009): Incremental dynamic analysis with consideration of modeling uncertainties. *Earthquake Engineering and Structural Dynamics*, **38** (6), 805-825.
- [10] Fischinger M, Kramar M, Isaković T (2009): Work package 1: Literature survey and identification of needs. Part 3: Design example. *SAFECAS-UL Report No. 3*, University of Ljubljana, Ljubljana, Slovenia.
- [11] CEN (2004): Eurocode 8: Design of structures for earthquake resistance – Part 1: General rules, seismic actions and rules for buildings. CEN, Brussels.
- [12] Zoubek B, Fischinger M, Isaković T (2016): Cyclic response of hammer-head strap cladding-to-structure connections used in RC precast building. *Engineering Structures*, **119**, 135-148.
- [13] McKenna F, Fenves GL (2010): Open System for Earthquake Engineering Simulation (OpenSees). Pacific Earthquake Engineering Research Center, Berkeley, USA.
- [14] Ibarra LF, Medina RA, Krawinkler H (2005): Hysteretic models that incorporate strength and stiffness deterioration. *Earthquake Engineering and Structural Dynamics*, **34** (12), 1489-1511.
- [15] Zoubek B, Fischinger M, Isaković T (2015): Estimation of the cyclic capacity of beam-to-column dowel connections in precast industrial buildings. *Bulletin of Earthquake Engineering*, **13** (7), 2145-2168.
- [16] Ugurhan B, Baker JW, Deierlein GG (2013): Incorporating model uncertainty in collapse reliability assessment of buildings. The 11th International Conference on Structural Safety and Reliability, New York, ZDA.
- [17] Babič A (2017): Seismic stress test for precast reinforced concrete buildings. Doctoral dissertation, University of Ljubljana, Ljubljana, Slovenia. (in Slovenian.)
- [18] Snoj J (2014): Seismic risk assessment of masonry buildings. Doctoral dissertation, University of Ljubljana, Ljubljana, Slovenia. (in Slovenian.)
- [19] Marinko S (2015): Cening 79 – Gradbena dela. Inženiring biro Marinko, Ljubljana, Slovenia. (in Slovenian.)
- [20] MOP (Ministry of the Environment and Spatial Planning) (2007): Pravilnik o spremembah in dopolnitvah Pravilnika o cenah in normativih za določanje cen gradbenih del za popotresno obnovo objektov. Uradni list RS, št. 83-4213/2007. (in Slovenian.)
- [21] Lapajne J, Šket Motnikar B, Zupančič P (2003): Probabilistic seismic hazard assessment methodology for distributed seismicity. *Bulletin of the Seismological Society of America*, **93** (6), 2502-2515.
- [22] Baker, JW (2011): Conditional Mean Spectrum: tool for ground motion selection. *Journal of Structural Engineering*, **137**: 322-331.
- [23] CEN (2019): Eurocode 8: Design of structures for earthquake resistance – Part 1-2: Rules for new buildings. Working draft version 3. CEN, Brussels.